

Sergio Caserta
Marino Simeone
Stefano Guido

A parameter investigation of shear-induced coalescence in semidilute PIB–PDMS polymer blends: effects of shear rate, shear stress volume fraction, and viscosity

Received: 22 July 2005
Accepted: 19 January 2006
Published online: 9 March 2006
© Springer-Verlag 2006

Paper presented at the Annual Meeting of the European Society of Rheology, Grenoble, April 2005.

S. Caserta (✉) · M. Simeone · S. Guido
Laboratori “Giovanni Astarita,”
Dipartimento di Ingegneria chimica,
Università degli Studi di Napoli
Federico II,
P. le V. Tecchio 80,
Napoli 80125, Italy
e-mail: scaserta@unina.it

Abstract In this work, drop coalescence of polymer blends under shear flow in a parallel flow apparatus was investigated by optical sectioning microscopy. In each experiment, shear rate was set at values low enough to avoid any break-up phenomena. The time evolution of the drop size distribution was determined by motorized sample scanning and iterative acquisition of stacks of images along sample depth. Drop size and location in the acquired images was found by automated image analysis techniques. A systematic experimental campaign to investigate the effects of shear rate (in the range $0.1\text{--}0.5\text{ s}^{-1}$), volume fraction (2.5–10%), and viscosity of the two phases (3–63 Pa s) at different viscosity ratio (0.1–2.3) was carried

out. By comparing data from different experiments, it was found that at any strain value, the average drop size decreases monotonically with the shear stress, calculated as the product of shear rate and matrix viscosity. Furthermore, the coalescence rate slowed down with increasing viscosity ratio. Overall, these results provide an extensive set of data, which can be used as a benchmark for modeling shear-induced coalescence in polymer blends.

Keywords Coalescence · Polymer blends · Morphology · Shear flow · Optical microscopy · Image Analysis

Introduction

The investigation of drop coalescence in polymer blends under controlled flow conditions has attracted much interest in the literature, both from the experimental and the theoretical side. Indeed, it is well known that coalescence plays an essential role on the flow-induced evolution of the drop size distribution, which is a key feature for the final properties of products obtained by industrial processing of polymer blends in the molten state.

From the theoretical standpoint, drop coalescence during flow was modeled (Chester 1991) by considering an external, macroscopic flow field and an internal microscopic one, corresponding to the draining of the interven-

ing film among two colliding drops. The external flow defines the mutual force and the interaction time between the two colliding drops and the collision frequency C (Smoluchowski 1917). In simple shear flow, in the case of equal-sized particles of diameter d , the collision frequency is proportional to the shear rate ($\dot{\gamma}$) and to the squared volume fraction of the dispersed phase, which is expressed as the number of drops per unit volume n

$$C \propto \dot{\gamma} \cdot d^3 \cdot n^2 \quad (1)$$

The internal flow can be used to give an estimate of the time needed to drain the liquid film between the drops. By

comparing the interaction time and the drainage time, it is possible to estimate the probability or efficiency that a drop collision leads to coalescence. In this framework, coalescence will happen if the interaction time is much bigger than the drainage time or if drop trajectories are such that the minimum distance among them is lower than some critical value (Vinckier et al. 1998).

By resorting to a different approach, Wang et al. (1994) considered how hydrodynamic interactions among drops induce deviations from the unperturbed trajectories. This theory should justify the fact that coalescence efficiency is also apparently dependent on the ratio between the size of the two colliding particles.

Rusu and Peuvrel-Disdier (1999) measured drop size evolution in flow conditions where no break-up was active. The dependence of the coalescence kinetics on shear rate step-down ratio and dispersed phase concentration was investigated. Good agreement was found with the predictions of the Chester model in terms of the dependence of the apparent steady state average drop size on the applied shear rate. The model, however, did not provide a satisfactory description of coalescence kinetics.

Recently (Lyu et al. 2002), shear-induced evolution of average drop size was studied both experimentally and theoretically. A population balance model taking into account the two competing processes of drop break-up, as described by single drop theories, and coalescence, as described by several models (Smoluchowski 1917; Wang et al. 1994; Chester 1991), was used for data fitting and interpretation. A comparison of calculations with experimental data shows that none of the coalescence models provides quantitative predictions of the coalescence kinetics. The observed trends show that coalescence efficiency decreases with increasing shear rate and that coalescence rate increases with increasing volume fraction in qualitative agreement with Eq. 1. Furthermore, a maximum of coalescence efficiency as a function of viscosity ratio was found.

As a matter of fact, one of the major experimental problems in investigating drop coalescence in nondilute biphasic mixtures is to obtain statistically significant and reproducible data due to the large number of drops that need to be examined. Automated methods are therefore in order.

Among the techniques typically used to characterize the morphology of a polymer blend, some are based on correlations between rheological properties of the blend, elastic and viscous modulus (G' , G'') in particular, and the morphology of the constitutive phases, or more specifically, the average drop diameter (Paliere 1990; Graebing 1993; Simeone 2002). The main limit of this technique is the need of very precise measurements of the shear moduli in a wide frequency range. Furthermore, these techniques allow us to determine the first moment only, rather than the whole drop size distribution. Light scattering can be used as an indirect measurement to characterize higher moments

of the drop size distribution in case drops are smaller than 10 μm (Rusu and Peuvrel-Disdier 1999).

Optical microscopy allows the direct observation of the sample and precise measurements of the whole drop size distribution in a noninvasive way. However, even in the case of transparent phases, microscopy images of polymer blends are difficult to handle due to the presence of strong out-of-focus components brought about by the drops lying above or below the focal plane. Owing to these difficulties, the direct measurements of drop size distributions by optical microscopy presented so far in the literature are either restricted to rather low dispersed phase concentration or often the result of laborious manual analyses of a limited number of drops.

In this work, a systematic experimental campaign on drop coalescence was carried out by exploiting a computer-controlled optical microscopy sectioning technique, which solves most of the above mentioned difficulties by allowing one to sample high number of drops in a fully automated fashion and to evaluate the statistical significance of the obtained results. The effect of relevant experimental variables, such as dispersed phase volume fraction, shear rate, and viscosity, was extensively investigated on a blend of Newtonian components [polyisobutene (PB) and polydimethylsiloxane (PDMS)] with the main objective to provide a set of data under controlled experimental conditions to be used as a benchmark for modeling work.

Experimental part

Materials

In all the experiments of this work, the system used was polyisobutene–polydimethylsiloxane, which is a pair of immiscible Newtonian model fluids widely used in the literature (Grizzuti and Bifulco 1997; Minale et al. 1997, 1998; Vinckier et al. 1998; Caserta et al. 2004). Polyisobutene (PB) was supplied by BP Chemicals under the trade names of Napvis or Indopol. Two different grades, i.e., Napvis 10 (or Indopol 100) and Napvis 30, having a viscosity of 27.3 and 83.3 Pa·s at 23°C, respectively, were used. Polydimethylsiloxane is a silicone oil (SO) supplied by Dow Corning, also available in several grades. In this work, two grades with nominal viscosity of 12 and 60 Pa·s were used.

Both PB and SO were liquid and transparent at room temperature. Refractive indices at 23°C, as measured by using an Abbe refractometer, were 1.40 for the SO and 1.50 for PB. Rheological tests were carried out in a constant-stress instrument (Bohlin CVO 120). By mixing different grades of the two polymers, fluids having different viscosities at 23°C were obtained (see Table 1). Both polymers exhibited Newtonian behavior in the range of shear rates investigated in the rheological characterization

Table 1 Overview of the experimental campaign

Exp	η_m (Pa s)	η_d (Pa s)	λ	σ (mN/m)	Φ (wt%)	γ (s^{-1})	τ (Pa)
A	27.4	26.8	0.98	2.10	2.50	0.33	9.0
B	27.4	26.8	0.98	2.10	5.00	0.33	9.0
C	27.4	26.8	0.98	2.10	10.00	0.33	9.0
D	46.8	48.5	1.04	1.35	5.00	0.10	4.7
E	10.5	10.3	0.98	1.30	5.00	0.50	5.3
F	27.5	27.5	1.00	1.72	5.00	0.50	13.8
G	46.8	48.5	1.04	1.35	5.00	0.32	15.0
H	46.8	48.5	1.04	1.35	5.00	0.50	23.4
I	27.4	2.7	0.10	2.20	4.93	0.50	13.7
J	27.4	63.4	2.31	1.30	5.00	0.50	13.7

(up to 10 s^{-1} , which is well above the shear rate imposed in the experiments): Viscosity was constant with shear rate and the first normal stress difference was so small as to fall below the sensitivity of the instrument.

The immiscibility of the two fluids has been tested by monitoring the diameter of a single drop of the dispersed phase immersed in the continuous one. In the case of our experiments, i. e., SO drop in PB matrix, no significant variation was detected on the time scale of the experiments, thus ensuring that the fluids can be considered as immiscible for the scope of this work. On the other hand, a small miscibility of a PB drop in a SO matrix was observed, in agreement with previous results (Guido and Villone 1998), and was attributed to the partial solubility of low molecular weight PB chains in the SO (Shi et al. 2004).

The interfacial tension between the two phases was measured by analyzing drop retraction after cessation of a shear flow, as reported by Guido and Villone (1998). The experiments were carried out on isolated drops of SO injected into the PB with a tiny glass capillary. The drop relaxation after cessation of flow was observed along the direction of the velocity gradient through the parallel plate apparatus described below. The analysis was based on the time evolution of the parameter D' , defined as $D'=(R_p-R_z)/(R_p+R_z)$ where R_p and R_z are the major and minor axis of the projection of the drop along flow direction. The following simple analytical expression for the evolution of D with time during retraction was used

$$D' = D'_0 \exp\left(-\frac{40(\lambda + 1)}{(2\lambda + 3)(19\lambda + 16)} \frac{t\sigma}{\eta_m R}\right) \quad (2)$$

where D'_0 is the value of D' at the beginning of the retraction. According to Eq. 2, data of $\ln(D'/D'_0)$ plotted vs time should fall on a straight line whose slope is proportional to σ . Equation 2 was obtained from the first-order theory of Taylor (1932) according to the formulation given by Rallison (1984) and is valid only in the limit of small deformations, hence, the fit was restricted to values of $D' \leq 0.15$. In this work, $\ln(D'/D'_0)$ was plotted as a

function of $t\sigma/\eta_m R$ for the retraction of several drops and σ was calculated as the average value of the fitting parameter (data are not shown here for the sake of brevity, but examples of this procedure can be found in Caserta et al. (2005a).

The details of the experiments presented in this work are summarized in Table 1.

Methods

Because a detailed description of the experimental technique, data analysis, and possible sources of errors was provided elsewhere (Caserta et al. 2004), only the main features will be briefly reviewed in this section. Simple shear flow was generated by a rheo-optical parallel plate apparatus that essentially consists of a parallel-plate device coupled with an optical microscope (Axioskop FS, Zeiss). The plates are two glass slides, each attached to a rigid mount, one of which is motorized along two perpendicular horizontal directions by means of a computer-controlled stepper motor (Ludl). Simple shear flow is generated by displacing the motorized glass slide with respect to the other, once the opposing glass surfaces were properly aligned by means of a set of rotary and tilting micrometric stages. The residual misalignment was typically less than $20\text{ }\mu\text{m}$ over the entire surface of the slides. The desired gap between the slides can be set by means of a vertical micrometric stage. In the experiments performed in this work, the gap was always set to $500\text{ }\mu\text{m}$.

Observations were performed in transmitted light by using a long working distance objective (20/0.40 Achromat) with an estimated depth of field of $3.23\text{ }\mu\text{m}$ (Inoue' 1986). The microscope itself was mounted on a motorized translating stage to allow for automated positioning. The sample was observed along the velocity gradient and images were captured with a B/W CCD video camera (KP-ME1, Hitachi) connected to the microscope. Due to the turbidity of the mixtures, an increasing image degradation was noticed by focusing inside the sample. All the experiments were performed in a room at controlled temperature of $23 \pm 0.5^\circ\text{C}$.

Experimental protocol

A biphasic mixture of the desired composition was prepared, carefully homogenized taking care to avoid air inclusions, then degassed under vacuum, and was left to equilibrate overnight. A few milliliters of the obtained blend were loaded between the parallel plates, which were brought to the desired distance, i.e., calc. $500\text{ }\mu\text{m}$, by squeezing the sample with the vertical stage. A preshear of 40 s^{-1} was applied to cancel loading effects and uniform the mixture morphology by breaking-up most of the drops; shear rate was stepped-down to a given value of the shear

rate (in the range 0.01 to 1 s^{-1}), which was kept fixed for the rest of the experiment. During shear flow, drop break-up was completely absent, as determined by direct optical observation of the sample during the experiment, and the only mechanism acting to modify the blend morphology was coalescence. Flow direction was inverted from time to time to limit the displacement between the plates. The maximum plate displacement imposed in the experiments was 6 cm.

At every inversion, the flow was stopped for a short time to allow for drop relaxation to the spherical shape. Because drop retraction and the following start-up transient of drop deformation upon resuming the flow took a few seconds (whereas the shearing time between two consecutive inversions was of the order of several hundreds of seconds), the influence of flow inversion on the overall strain (strain=shear rate \times flow time) experienced by the sample can be regarded as negligible. Several tests were performed to evaluate the effect of the flow inversion and other possible sources of experimental error (Caserta et al. 2004). It was concluded that the methodology is reliable and provides a good reproducibility of the results.

Shear flow was stopped periodically to acquire images to be used to characterize the morphology of the sample at the current time. As soon as the drops had relaxed to a spherical shape, sets of images were captured and stored on hard disk for later analysis. To evaluate possible wall effects and imaging artifacts, a 3-D computer-controlled sample scanning was performed. To this purpose, images of layers at increasing depth in the sample were acquired by gradually changing the microscope focus through the motorized drive. In such optical sectioning procedure, the distance between consecutive layers (around 3 μm) was set below the depth of field of the lens used. About ten such stacks (each made up of calc. 100 images) were automatically taken by translating the microscope and iterating the sectioning procedure. The overall time required by sample scanning and image acquisition was about 15–20 min.

Data analysis

Image analysis techniques were used to automatically detect drop size and position in each stack. A fully automated software (Caserta et al. 2004, 2005b) allowed us to process a large number of images, typically corresponding to a few thousands of drops (which would be a cumbersome task if carried out manually), and to reconstruct the 3-D microstructure of the sample because both size and position of each drop are determined.

One of the main problems in data analysis is to evaluate whether the region of the sample optically sectioned can be considered as representative of the whole blend or, in other words, how many drops need to be measured to get statistically significant results. The random sampling error

was calculated according to theoretical predictions, taking into account the measured size distribution of the sample and the number of inclusions measured (Paine 1993). This way, it was possible, for example, to have an estimate of the error associated with the average or the variance of the size distribution. To limit this error to less than 10%, the sample size, i.e., the number of drops to be measured, was often of the order of several thousands, depending on the variance of the distribution. It must be noted that the estimate of the random sampling error is valid only if the sample size is bigger than a critical value, which depends itself on the variance of the distribution and can easily be of the order of magnitude of thousands of drops (Paine 1993). If this is not the case, the error can be significantly underestimated and the data analysis cannot be considered statistically valid. In all the experiments presented in this work, the random sampling error was usually below 5% and always less than 10%.

Results

The main objective of this work was to perform a parametrical investigation of coalescence kinetics. To this end, several experiments were run by keeping all the parameters constant except for one whose influence was investigated by calculating the Sauter average drop

diameter $D_{3,2} = \frac{\sum_{i=1}^N n_i d_i^3}{\sum_{i=1}^N n_i d_i^2}$ as a function of strain. The choice

of a volume-based average size is in line with most studies in the literature and can be regarded as more reliable compared to the average number because analysis of the larger drops is more accurate (Burkhart et al. 2001).

In spite of the preshear step, a slight residual difference in the initial values of the average drop size was found in all the experiments. Therefore, for the sake of comparison, the average diameter $D_{3,2}$ was made nondimensional with respect to a common starting value $D_{3,2}^0$ for the different experiments. In other words, the time at which $D_{3,2}$ reached the value $D_{3,2}^0$ was taken as the origin of the time scale of each experiment.

The possible influence of sedimentation during the shearing experiment was checked by dividing the stacks in several subregions along the sample thickness and measuring the average drop size in each subregion as a function of strain (Caserta et al. 2004, 2005a,b). The data calculated superimpose within the experimental error for most of the experimental run, some deviations becoming significant in a few samples only at the highest values of strain. The sedimentation test was performed on all the experiments and all the data points starting from the strain value where a significant difference between the subregions of the sample was measured were discarded from further analysis. It should be also noticed that despite the

fact that the experiments were run up to 70,000 strain units, no apparent steady state morphology was observed (only a slowing down of the coalescence kinetics was found).

Effect of volume fraction

In Fig. 1, three experiments (Exp A, B, and C) run on the SO in PB polymer blend are presented. The only difference among the three experiments is the dispersed phase wt fraction Φ . In fact, data show a strong influence of Φ on the coalescence kinetics. This can be attributed (Chester 1991) to the fact that the collision frequency scales with the volume fraction Φ of the dispersed phase to the second power (Eq. 1). In the concentration range investigated in this work, data support this interpretation, as shown in Fig. 2 where the drop diameter evolution for the three experiments is plotted vs the quantity strain $\times\Phi^2$. Similar results were found by Vinckier et al. (1998). Rusu and Peuvrel-Disdier (1999) found that of the average drop size does not depend on the concentration, but their results apply to the apparent steady state value in a more viscous system.

It was shown that at early times in the coalescence kinetics, data are in good agreement with the predictions of the Smoluchowski theory when the average drop diameter is plotted as a function of strain times the volume fraction (Lyu et al. 2000; Burkhart et al. 2001; Lyu et al. 2002). Such plot is shown in the inset of Fig. 2. It can be seen that in line with previous results, data superimpose somehow at the beginning (some scatter can be attributed to the already mentioned uncertainty in the starting time) and then deviate at some point from this common trend. It can be concluded that the scaling with the square concentration is not valid throughout the coalescence process, but gives a reasonable representation of data at later times.

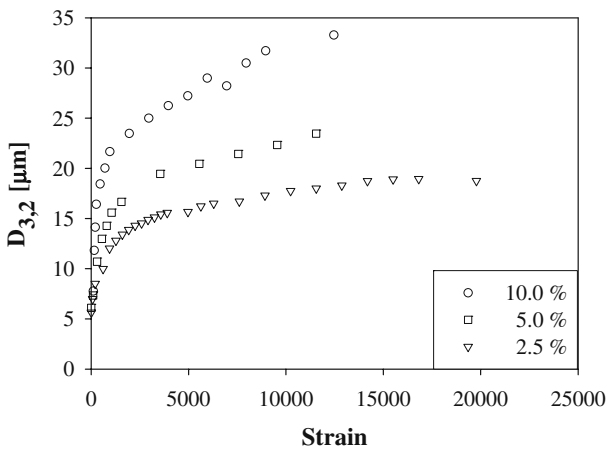


Fig. 1 Matrix phase I100, dispersed phase 39.7wt% SO 60000–60.3wt% SO 12500, $\dot{\gamma} = 0.33 \text{ s}^{-1}$, $\eta_m = 27.4 \text{ Pa s}$, $\lambda = 0.98$, and $\sigma = 2.1 \text{ mN/m}$. Evolution of Sauter mean diameter with strain, parametric in the dispersed phase wt fraction

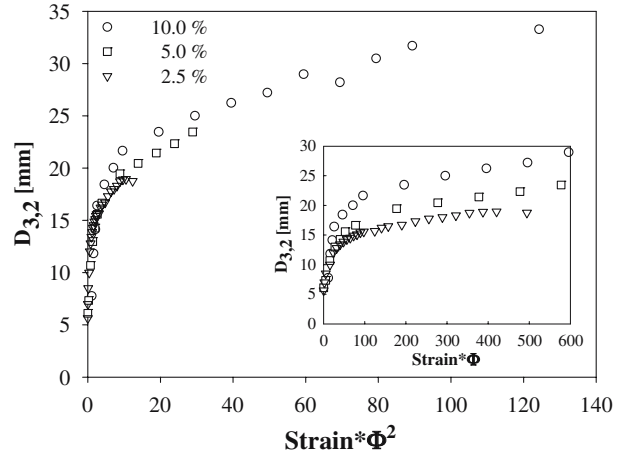


Fig. 2 Volume fraction scaling. Same data as in Fig. 1

Effect of shear rate, viscosity, and shear stress

The effect of flow intensity on coalescence was investigated by performing experiments at different values of shear rate. In Fig. 3, the average diameter $D_{3,2}$ normalized with respect to the common initial value ($D_{3,2}^0 = 12.3 \mu\text{m}$), is plotted as a function of strain for the experiments D , G , and H in the $\dot{\gamma}$ range from 0.1 to 0.5 s^{-1} . The data in Fig. 3 show that the lower the shear rate is, the faster is the coalescence process, a result that can be attributed to the increase of drainage times with drop deformation (Chester 1991). In fact, lower shear rate are associated with less deformed drops and smaller interfacial regions of close approach where the intervening film of the continuous phase is squeezed by the external flow. In such conditions, less resistance is encountered in film drainage compared to the case of higher drop deformations.

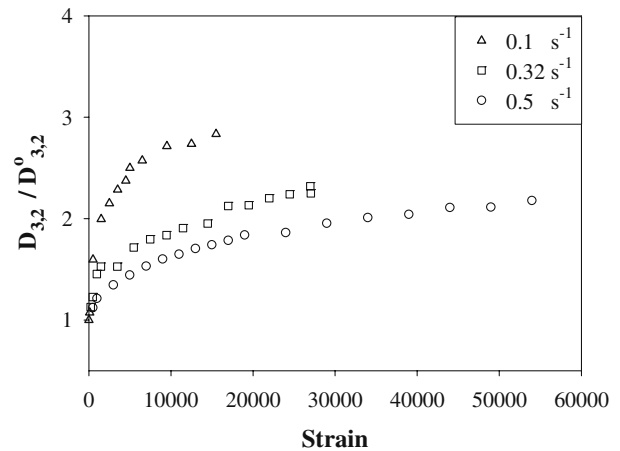


Fig. 3 Matrix phase 50.3wt% I100–49.7wt% N30, disperse phase 80.28wt% SO 12500–19.71wt% SO 60000, $\eta_m = 46.8 \text{ Pa s}$, $\lambda = 1.04$, $\sigma = 1.35 \text{ mN/m}$, and $\Phi = 5\%$. Evolution of the normalized Sauter average drop diameter ($D_{3,2}^0 = 12.4 \mu\text{m}$) parametric in shear state

The influence of matrix viscosity alone on the coalescence rate was also independently investigated. In Fig. 4, the evolution of the Sauter average diameter, normalized with respect to its initial value ($D_{3,2}^0 = 12.3 \mu\text{m}$), is compared for three experiments (Exp E, F, and H) on different SO/PB blends. In all the experiments, $\lambda=1$, $\Phi=5\%$, and $\dot{\gamma}=0.5 \text{ s}^{-1}$, but the values of the viscosity of the two phases are different (matrix viscosity is 10.5, 27.5, and 46.8 Pa s). It should be noted that the different composition of the three blends is associated with slightly different values of interfacial tension (see Table 1), possibly due to experimental error (the nominal value of 1.3 mN/m is reported in the figure caption). However, we believe that these differences are negligible compared to the effect of viscosity, which is mainly responsible for the differences found in the experiments.

The coalescence was slowed down in the case of higher viscosity, in agreement with the fact that the higher the matrix viscosity, the slower the drainage of the film between two colliding drops, hence decreasing coalescence efficiency. It should be noticed that the three experimental curves in Fig. 4 start from the common value of the average Sauter diameter ($D_{3,2}^0 = 12.3 \mu\text{m}$), but from different values of the average Capillary number due to the difference in the viscosity.

The data presented in Figs. 3 and 4 were replotted as parametric in the external shear stress $\tau = \eta_m \times \dot{\gamma}$ in Fig. 5. In fact, in our experiments we impose the shear rate, hence τ is the imposed stress calculated according to the matrix viscosity (i.e., neglecting the difference between the viscosity of the matrix and the viscosity of the blend). It can be noticed that higher values of the shear stress are associated with slower coalescence rates. Thus, the viscosity and shear rate dependence of the coalescence rates can somehow be incorporated into the shear stress as shown by the monotonic trend in Fig. 5. In fact, by plotting

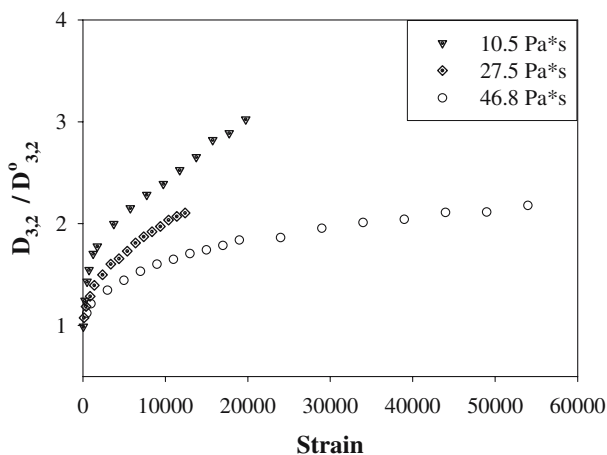


Fig. 4 Evolution of the normalized Sauter average drop diameter with strain parametric in η_m . ($D_{3,2}^0 = 12.3 \mu\text{m}$, $\lambda = 1.04$, $\sigma = 1.3 \text{ mN/m}$, $\Phi = 5\%$, $\dot{\gamma} = 0.5 \text{ s}^{-1}$)

$D_{3,2}$ as a function of shear stress at a given value of strain, we found that data follow a linear trend in log-log scale (the plot is not shown for the sake of brevity).

In Figs. 6 and 7, the drop size distributions of the experiments presented in Fig. 5 are presented. The data are plotted as cumulative numeric distributions F at strains 1,000 and 10,000. Dressler and Edwards (2004), on the basis of a Hamiltonian framework model, predict that the dispersity of the drop size distribution is affected by shear flow. In our experimental campaign in pure coalescence regime, we found that the dispersity of the blend increases with time during flow as shown by of the spreading of the drop size distribution from strain 1,000 to 10,000 in each experiment. By increasing τ the whole drop size, distribution shifts to the left and is characterized by a smaller variance.

Effect of viscosity ratio

The effect of the viscosity ratio $\lambda = \eta_d / \eta_m$ was also investigated. In Fig. 8, three separate experiments (Exp F, I, and J) with λ equal to 0.1, 1, and 2.38 are compared. All the experiments were run at a shear rate of 0.5 s^{-1} with a dispersed phase volume fraction of 5%. The matrix phase (PB) had a viscosity of 27.4 Pa s and the viscosity ratio was changed by mixing different SO grades in the preparation of the dispersed phase. The data in Fig. 8 show that the lower the viscosity ratio is, the faster the coalescence kinetics. A possible explanation of this result is that in the case of low viscosity ratio, the flow of the intervening film of the continuous phase could be somehow affected by the development of internal circulations in the colliding drops. The corresponding drainage flow of the matrix film will then be characterized by a flatter velocity profile that will reduce the viscous losses.

To study the dependence of the drop coalescence kinetics on the viscosity ratio, we followed the same

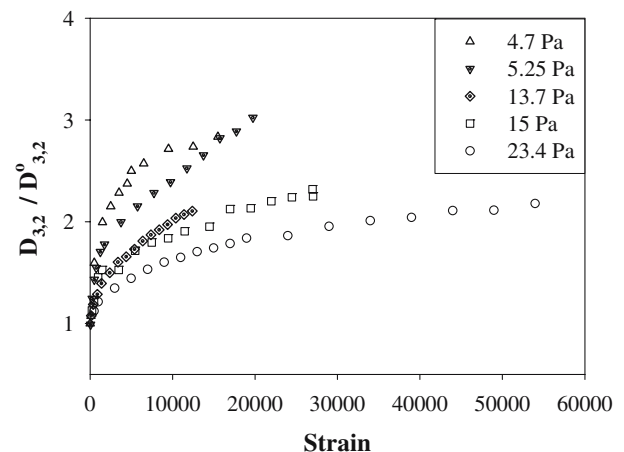


Fig. 5 Shear stress scaling. Same data as in Figs. 3 and 4

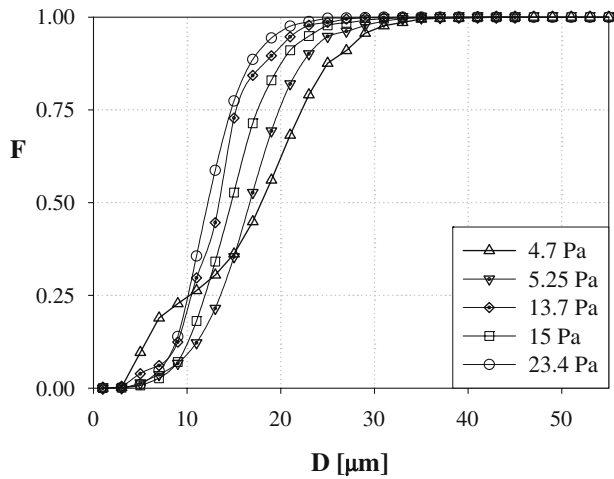


Fig. 6 Drop size distribution of experiment in Fig. 5 at strain 1,000

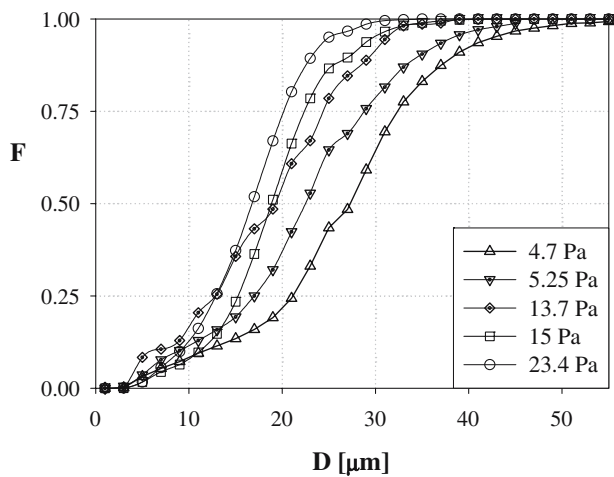


Fig. 7 Drop size distribution of experiment in Fig. 5 at strain 10,000

procedure used for the data in Fig. 6. By plotting $D_{3,2}$ as function of λ at fixed values of strain on a log–log scale, we found that the data follow a linear trend (the plot is not reported here for the sake of brevity). The three fitting lines were not parallel but rather converging to a single point. This trend can be simply interpreted in terms of the reduced coalescence rate at higher viscosity ratio. This finding, however, is at variance with the results of Lyu et al. (2000, 2002) who explored a range of viscosity ratios between 0.003 and 2.6 at fixed shear rate, matrix viscosity, and volume fraction and who found a maximum in coalescence efficiency at λ close to one. A possible explanation for this discrepancy could be that the maximum in coalescence efficiency for PDMS–PIB blends is shifted toward lower values of viscosity ratio.

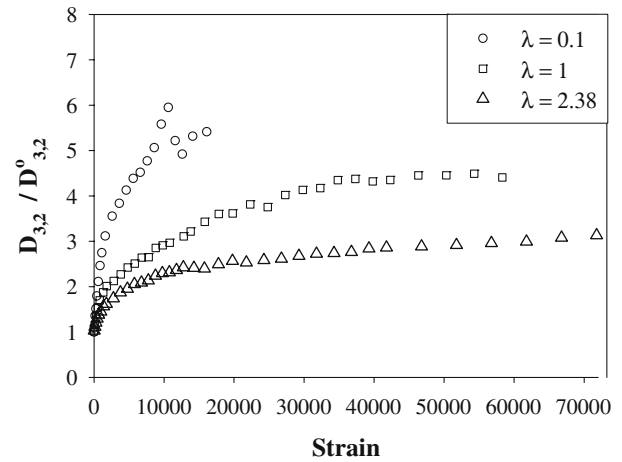


Fig. 8 Influence of viscosity ratio on the coalescence kinetics ($D_{3,2}^0 = 8.1 \mu\text{m}$, $\Phi = 5\%$, $\eta_m = 27.4 \text{ Pa}\cdot\text{s}$, $\dot{\gamma} = 0.5 \text{ s}^{-1}$)

Conclusions

In this work, an extensive parameter investigation was experimentally performed to examine the influence of relevant variables on the coalescence rate of semidilute PB–SO blends sheared in a parallel plate apparatus. The morphology evolution during flow was characterized by means of an automated experimental technique based on optical sectioning and offline image analysis.

The experimental campaign was designed to isolate the effect of single physical parameters on the evolution of drop size distribution due to coalescence only. The main results of this work can be summarized as follows. Concerning the effect of dispersed phase volume fraction, we found that coalescence rate increases with volume fraction. Apart from the initial region of steep growth, data are well represented when the average drop size is plotted vs $\text{strain} \times (\text{volume fraction})^2$. Concerning the effect of flow intensity, we found that the effect of shear rate and matrix viscosity can be described in terms of shear stress only. The lower the shear stress is, the faster is the coalescence process, a result that can be attributed to the increase of drainage times with drop deformation or with matrix phase viscosity (Chester 1991). Finally, lower drop phase viscosity (at constant matrix viscosity) resulted in faster coalescence rate in a monotonic fashion.

Acknowledgement Helpful discussion with Dr. Francesco Greco is gratefully acknowledged.

References

- Burkhardt BE, Gopalkrishnan PV, Hudson SD, Jamieson AM, Rother MA, Davis RH (2001) Droplet growth by coalescence in binary fluid mixtures. *Phys Rev Lett* 87:983041–983044
- Caserta S, Simeone M, Guido S (2004) Evolution of drop size distribution of polymer blends under shear flow by optical sectioning. *Rheol Acta* 43: 491–501
- Caserta S, Sabetta L, Simeone M, Guido S (2005a) Shear induced coalescence in aqueous biopolymer systems. *Chem Eng Sci* 60:1019–1027
- Caserta S, Simeone M, Guido S (2005b) 3D optical sectioning and image analysis of particles in biphasic systems. *Microsc Anal* 19:9–11
- Chester AK (1991) The modelling of coalescence processes in fluid–liquid dispersions: a review of current understanding. *Trans Inst Chem Eng* 69: 259–270
- Dressler M, Edwards BJ (2004) Rheology of polymer blends with matrix-phase viscoelasticity and a narrow droplet size distribution. *J Non-Newton Fluid Mech* 120:189–205
- Graebing D, Muller R, Palierno JF (1993) Linear viscoelastic behavior of some incompatible polymer blends in the melt: interpretation of data with a model of emulsion of viscoelastic liquids. *Macromolecules* 26:320–329
- Grizzuti N, Bifulco O (1997) Effect of coalescence and breakup on the steady state morphology of an immiscible polymer blend in shear flow. *Rheol Acta* 36:406–415
- Guido S, Villone M (1998) Three dimensional shape of a drop under simple shear flow. *J Rheol* 42:395–415
- Inoue S (1986) *Video microscopy*. Plenum, New York
- Lyu S, Bates F, Macosko CW (2000) Coalescence in polymer blends during shearing. *AIChE J* 46:229–238
- Lyu S, Bates F, Macosko CW (2002) Modeling of coalescence in polymer blends. *AIChE J* 48:7–14
- Minale M, Moldenaers P, Mewis J (1997) Effect of shear history on the morphology of immiscible polymer blends. *Macromolecules* 30:5471–5475
- Minale M, Mewis J, Moldenaers P (1998) Study of the morphological hysteresis in immiscible polymer blends. *AIChE J* 44:943–950
- Paine AJ (1993) Error estimates in the sampling from particle size distributions. *Part Part Syst Charact* 10:26–32
- Palierno JF (1990) Linear rheology of viscoelastic emulsions with interfacial tension. *Rheol Acta* 29:204–214
- Rallison JM (1984) The deformation of small viscous drops and bubbles in shear flows. *Annu Rev Fluid Mech* 16:45–66
- Rusu D, Peuvrel-Disdier E (1999) In situ characterization by small angle light scattering of the shear induced coalescence mechanism in immiscible polymer blends. *J Rheol* 43:1391–1409
- Shi T, Ziegler VE, Welge IC, An L, Wolf BA (2004) Evolution of the interfacial tension between polydisperse “immiscible” polymers in the absence and in the presence of a compatibilizer. *Macromolecules* 37:1591–1599
- Simeone M, Molè F, Guido S (2002) Measurement of average drop size in aqueous mixtures of Na-alginate and Na-caseinate by linear oscillatory tests. *Food Hydrocoll* 16(5):449–459
- Smoluchowski MV (1917) Versuch einer mathematischen theorie der Koagulationskinetik Kollider Losungen. *Z Phys Chem* 92:129–168
- Taylor GI (1932) The viscosity of a fluid containing small drops of another fluid. *Proc R Soc Lond A* 138:41–48
- Vinckier I, Moldenaers P, Terracciano AM, Grizzuti N (1998) Droplet size evolution during coalescence in semiconcentrated model blends. *AIChE J* 44:951–958
- Wang H, Zinchenko AZ, Davis RH (1994) The collision rate of small drops in linear flow fields. *J Fluid Mech* 261:161–88